Tellus SERIES B CHEMICAL AND PHYSICAL METEOROLOGY
PUBLISHED BY THE INTERNATIONAL METEOROLOGICAL INSTITUTE IN STOCKHOLM

Sulphate and chloride aerosols during Holocene and last glacial periods preserved in the Talos Dome Ice Core, a peripheral region of Antarctica

By YOSHINORI IIZUKA[1]*, BARBARA DELMONTE[2], IKUMI OYABU[1], TORBJÖRN KARLIN[3], VALTER MAGGI[2], SAMUEL ALBANI[2], MANABU FUKUI[1], TAKEO HONDOH[1] and MARGARETA HANSSON[3], [1]*Institute of Low Temperature Science, Hokkaido University, Sapporo, Japan;* [2]*Department of Earth and Environmental Sciences, University Milano-Bicocca, Milano, Italy;* [3]*Department of Physical Geography and Quaternary Geology, Stockholm University, Stockholm, Sweden*

(Manuscript received 1 December 2012; in final form 7 March 2013)

ABSTRACT

Antarctic ice cores preserve the record of past aerosols, an important proxy of past atmospheric chemistry. Here we present the aerosol compositions of sulphate and chloride particles in the Talos Dome (TD) ice core from the Holocene and Last Glacial Period. We find that the main salt types of both periods are NaCl, Na_2SO_4 and $CaSO_4$, indicating that TD ice contains relatively abundant sea salt (NaCl) from marine primary particles. By evaluating the molar ratio of NaCl to Na_2SO_4, we show that about half of the sea salt does not undergo sulphatisation during late Holocene. Compared to in inland Antarctica, the lower sulphatisation rate at TD is probably due to relatively little contact between sea salt and sulphuric acid. This low contact rate can be related to a reduced time of reaction for marine-sourced aerosol before reaching TD and/or to a reduced post-depositional effect from the higher accumulation rate at TD. Many sulphate and chloride salts are adhered to silicate minerals. The ratio of sulphate-adhered mineral to particle mass and the corresponding ratio of chloride-adhered mineral both increase with increasing dust concentration. Also, the TD ice appears to contain $Ca(NO_3)_2$ or $CaCO_3$ particles, thus differing from aerosol compositions in inland Antarctica, and indicating the proximity of peripheral regions to marine aerosols.

Keywords: aerosol compounds, ice sublimation method, marine aerosol, paleo-environmental reconstruction, sea-salt sulphatisation

1. Introduction

Aerosols are of central importance for atmospheric chemistry and physics, the biosphere and climate (Pöschl, 2005). Atmospheric aerosol particles in the free troposphere have a strong influence on direct and indirect radiation effects in the Earth's atmosphere (Andreae, 1995). The primary parameters that determine the environmental effects of aerosol particles are their concentration, size, shape, structure and chemical composition (Pöschl, 2005). These parameters, however, are spatially and temporally highly variable due to the aerosol having multiple sources. For example, primary aerosol particles are formed by the disintegration of bulk material on the Earth's surface (e.g. marine biota, sea salt and dust), whereas secondary aerosols are produced by chemical reactions in the atmosphere.

Antarctic ice cores preserve past aerosols, which are important proxies for past atmospheric chemistry (Legrand and Delmas, 1988; Legrand et al., 1988). Most of the more detailed information on aerosol deposition in Antarctica on glacial–interglacial timescales stems from ice cores drilled on the Central East Antarctic Plateau (CEAP), including Vostok (Petit et al., 1999), EPICA Dome C (EDC) (Wolff et al., 2006; Lambert et al., 2008) and Dome Fuji (DF) (Fujii et al., 2003; Watanabe et al., 2003). These interior sites have similar snow accumulation rates; moreover, for the insoluble dust, they also have similar sources, similar depositional fluxes and similar changes in magnitude over glacial–interglacial cycles (Delmonte et al., 2004a, 2004b, 2008).

*Corresponding author.
email: iizuka@lowtem.hokudai.ac.jp

Tellus B 2013. © 2013 Y. Iizuka et al. This is an Open Access article distributed under the terms of the Creative Commons Attribution-Noncommercial 3.0 Unported License (http://creativecommons.org/licenses/by-nc/3.0/), permitting all non-commercial use, distribution, and reproduction in any medium, provided the original work is properly cited.

Citation: Tellus B 2013, **65**, 20197, http://dx.doi.org/10.3402/tellusb.v65i0.20197

For soluble salts, the DF region of CEAP shows that the main salt components depend on the climate conditions. In warm periods, the main component is sodium sulphate, but in cold periods, they are sodium chloride and calcium sulphate (Iizuka et al., 2012a). In the present (late Holocene) climate, the most common aerosols in CEAP come from sea salt (sodium chloride) and marine biological activity (methansulphonic and sulphuric acids) in the Southern Ocean. These compounds then combine in the atmosphere to form sodium sulphate (Legrand and Delmas, 1988; Legrand et al., 1988). In the DF region, more than 90% of the initial sea salt becomes sulphatised in the first year after being precipitated (Iizuka et al., 2012b), indicating that almost all soluble salt in DF Holocene ice came from secondary aerosols.

On the other hand, the contribution of secondary aerosols to the total soluble aerosols probably differs in the Antarctic peripheral regions. Peripheral regions are located near the southern oceans, where marine aerosols (sea salt and biological activity) are likely to remain as primary aerosols and not undergo chemical reactions. To better understand past atmospheric chemistry throughout Antarctica, we also need to study the soluble salts in these marginal areas of the plateau.

Talos Dome (72°48′S, 159°06′E, 2315 m a.s.l.), hereafter TD, is a peripheral dome located in the South Pacific/Ross Sea sector of the East Antarctic Plateau (http://www.taldice.org/), drilled by the Talos Dome Ice Core drilling project (TALDICE). The uppermost 1550 m of the 1620-m deep TALDICE ice core provides a continuous record of paleoclimate for the Ross Sea sector of East Antarctica, covering the past 250 000 yr (Stenni et al., 2011). Because of the geographic location of the drilling site, there is a relatively high average snow accumulation rate of 80 kg m^{-2} yr^{-1} at present (Buiron et al., 2011; Schüpbach et al., 2011).

Compared to CEAP sites such as Dome C, the insoluble dust flux variability at TD during the last glacial–interglacial climate transition was considerably smaller in magnitude and decreased over the last 8–9 kyr (Albani et al., 2012). The different magnitude of dust flux variations and complementary geochemical evidence (Delmonte et al., 2010a, 2010b, 2013) indicate that the dust sources and the dynamics of atmospheric transport differ between the two sites, at least during the Holocene. Such specific behaviour of mineral dust at TD, mostly related to the atmospheric and climate history of the Western Ross sea embayment, also suggests that soluble salts in the TD region may reflect a different environmental history than the CEAP sites. For example, Sala et al. (2008) detected the presence of calcium carbonates such as calcite ($CaCO_3$), monohydrocalcite ($CaCO_3 \cdot H_2O$) and ikaite ($CaCO_3 \cdot 6H_2O$). Although the hydrous carbonates at TD, such as ikaite, likely originate from the sea ice surface (e.g. Sala et al., 2008), the calcite probably originates from terrestrial materials of local origin. In contrast, calcite is rarely found at inland sites such as DF (Kawamura et al., 2003; Iizuka et al., 2008).

Here, we present the compositions of soluble particles in TD ice core samples from several periods during the Holocene and Last Glacial Period (LGP), focusing on sulphate and chloride salts. Our particle extraction method involves ice sublimation (Iizuka et al., 2009). We then discuss the characteristics of soluble salts at the TD region from the LGP through the Holocene.

2. Experimental method

The TD samples were transported in the frozen state from the Milano-Bicocca cold-storage facility to a cold laboratory at the Department of Physical Geography and Quaternary Geology, Stockholm University (Sweden). There, they were preserved at temperatures of −25°C, which is below the eutectic temperatures of sodium sulphate, calcium sulphate and sodium chloride salts. We selected five samples from the Holocene, specifically three from the Late Holocene (2.7 kyrBP) and two from the Early Holocene (8.2 kyrBP), and six samples from the LGP, three of them dating around 27.1 kyrBP, which is near the Last Glacial Maximum (LGM), and the other three samples around 50.6 kyrBP (Buiron et al., 2011). The dating uncertainties are less than 0.3 kyr (Buiron et al., 2011). The accumulation rates were about 6.8, 5.9, 3.2 and 5.7 cm/year for the four time periods 2.7, 8.2, 27.1 and 50.6 kyrBP (Buiron et al., 2011). According to Albani et al. (2012), the concentration of dust particles of diameter 1–5 μm varied between periods and even during a period. For example, in the 8.2-kyr sample of the Holocene, the dust concentration was 67.4 ppb, which is much higher than the 7.0 ppb of the later Holocene sample at 2.7 kyr (Albani et al., 2012). The early Holocene was also colder than the later Holocene. On the other hand, the LGP dust concentrations were larger on average, being 179.2 ppb at 27.1 kyr and 81.1 ppb at 50.6 kyr.

For the aerosol-particle analysis, we pulverised a 1-g ice sample from the bottom 5-cm depth of each sample and sublimated the ice on a polycarbonate filter at −40°C using clean, dry air (Iizuka et al., 2009). The 5-cm thickness corresponds to 0.6 yr if we use the accumulation rate of 8 cm/yr of the late Holocene, or to 1.7 yr if we use the 3 cm/yr of the LGM (Buiron et al., 2011). The sublimation removes volatiles such as H_2O, HCl, HNO_3 and H_2SO_4. We sublimated 11 filter samples (Table 1) at Stockholm University and analysed them using scanning electron microscopy/energy dispersive spectroscopy (SEM-EDS: JSM-6360LV (JEOL) SEM & JED2201 (JEOL) EDS)

Table 1. Sample depth, age, total measured numbers and average size of non-volatile particles in 11 ice samples

Taldice Section no.	Measured Depth top (m)	Measured Depth bottom (m)	Climatic period	Age (kyrBP)	Averaged age	Total measured Number (N)	Average Diameter (μm)
226-b1	225.70	225.75		2.7		411	1.2
229-b1	228.70	228.75	late Holocene	2.7	2.7	522	0.9
232-b1	231.70	231.75		2.8		490	1.4
517-b2	516.95	517.00	early Holocene	8.1	8.2	483	0.9
519-b2	518.95	519.00		8.2		341	0.8
915-b1	914.70	914.75		27.0		525	1.1
917-b1	916.70	916.75	LGM (MIS2)	27.1	27.1	450	1.2
918-b1	917.70	917.75		27.2		364	1.0
1192-b2	1191.95	1192.00		50.3		356	1.2
1193-b2	1192.95	1193.00	LGP (MIS2)	50.6	50.6	479	0.9
1195-b2	1194.95	1195.00		50.8		469	1.1

Ages are cited from Buiron et al., 2011 and Schüpbach et al., 2011.

at the Institute of Low Temperature Science, Hokkaido University (Japan). Each filter yielded several hundred particles exceeding 0.4-μm in diameter, making a total of 4891 particles such as those shown in Fig. 1. Using SEM-EDS at 20 keV, we determined the levels of O, Si, Al, S, Cl, Na, Mg and Ca. The SEM-EDS method cannot accurately detect light elements such as C and N; moreover, C is contaminated from the polycarbonate filter.

To determine the sulphate, chloride and mineral components, we used the scheme in Iizuka et al. (2009) for identifying the non-volatile particles and separating the non-volatiles into soluble and insoluble components. Particles containing Si were assumed to have silicate material. About 99% of the S and Cl in the non-volatile particles are from soluble materials. As the sublimation removed the HCl and H_2SO_4, the S and Cl in the non-volatile particles were then assumed to be from sulphate and chloride salts. After considering the possible remaining compounds, we could assume that Na and S in a given particle came from Na_2SO_4, whereas Na and Cl came from NaCl. In a similar way, Ca and S came from $CaSO_4$, Mg and S from $MgSO_4$, Ca and Cl from $CaCl_2$, and Mg and Cl from $MgCl_2$.

We calculated the molar ratios of Na_2SO_4 to NaCl, $CaSO_4$ to Na_2SO_4 following the method described in Iizuka et al. (2012a). To determine m_{NaCl}, the mass of NaCl, we used our measure of m_{Na} and m_{Cl} to determine the number of ions N of each component. Then we assumed that the number of NaCl molecules equalled the minimum of N_{Na} and N_{Cl}. We followed the same method for the Na_2SO_4 and $CaSO_4$ salts. For reasons discussed in the next section, we included m_{MgSO_4} with $m_{Na_2SO_4}$ and m_{MgCl_2} with m_{NaCl}. The molar ratios were reproducible (twice-measured on the same filter) when we excluded particles with diameters exceeding three standard deviations above the average diameter. Such huge particles were excluded from the molar calculations.

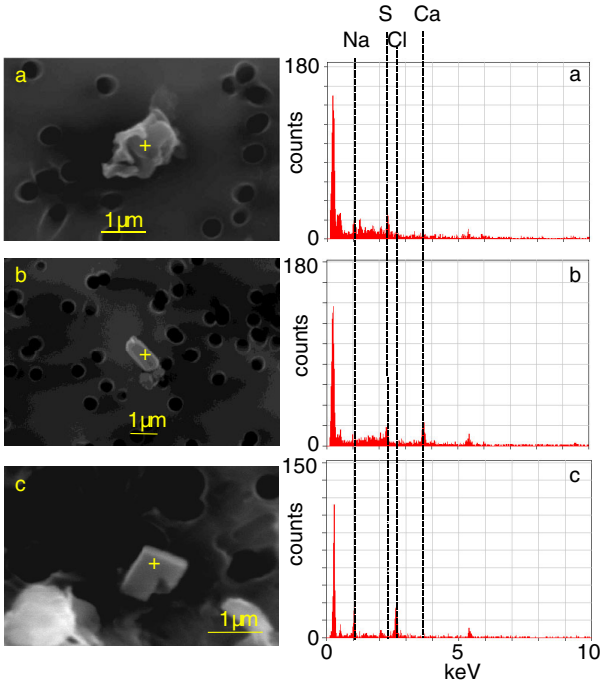

Fig. 1. photomicrographs and elements of typical particles in the filter samples. (a) Sodium sulphate from sample number 226_b1 (see Table 1 for depth of each sample). (b) Calcium sulphate from sample 1193_b1. (c) Sodium chloride from sample 1195_b1. Filters are 13-mm in diameter, made from polycarbonate, with a pore size of 0.4 μm (Advantec, K040A013A). All filters were coated with platinum for 30 s with a thickness of 10 nm using magnetron sputtering (Vacuum Device, MSP-10). The images were taken with the following settings: scanning time 80 s; space resolution 1280 × 960 pixels; spot size 45.

3. Results and discussion

3.1. Comparison of number and molar ratios of Na_2SO_4 to NaCl, $CaSO_4$ to Na_2SO_4.

Figure 2 shows the molar and number ratios of Na_2SO_4 to NaCl and the same for $CaSO_4$ to Na_2SO_4 for the 11 samples. For each set of compounds, the molar ratio nearly equals the number ratio. Thus, one can use the number ratio to estimate the molar (or mass) ratio of these compounds. The main factors that influence the calculated number and molar ratios are the atomic ratio and diameter of each particle. Therefore, the equality of the two ratios may be due to the averaging over all the particles on a given filter sample.

3.2. Comparison of chemical components of soluble particles between Holocene and LGP in TD and DF ice cores

The number fractions of particles containing sulphate and/or chloride salts in the 11 samples average 0.624 (i.e. 62.4%) of the total particles (Fig. 3). No significant difference occurs between the stages at 2.7, 8.2, 27.1 and 50.6 kyrs. This suggests that sulphate and chloride salts are the main soluble aerosols of TD ice. Also, the relationship with dust concentration (Fig. 4) shows no significant difference between the four stages, which indicates that the number fractions are probably independent of climate during the last 50 kyr.

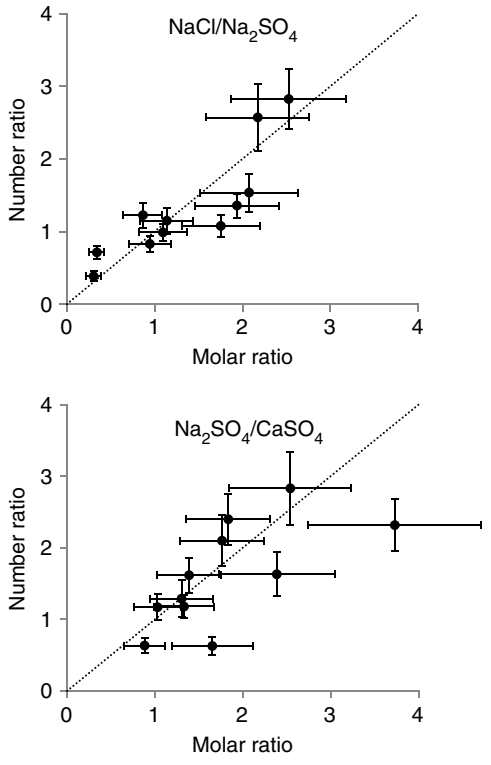

Fig. 2. Number and molar ratios of sodium and calcium compounds in 11 TD samples. (top) $NaCl/Na_2SO_4$. (bottom) $Na_2SO_4/CaSO_4$. Dotted lines show the 1:1 relation. Errors for the number ratio were calculated using the method in Iizuka et al. (2009), whereas those for mass ratio used the method in Iizuka et al. (2012b).

On the other hand, the number fraction of particles containing silicate minerals increases with increasing dust concentration, as shown in Fig. 4. This means that a higher contribution of dust (Si) to total particles occurs at higher dust concentrations. At 2.7 yr (early Holocene), about 75% of the particles contain dust, but at 27.1 kyr (LGM), the percentage rises to about 90%.

We now examine the number fraction of sulphate particles adhered with dust to total sulphate particles, or the sulphate coexistence ratio, and the corresponding ratio for chloride. Both such ratios increase with increasing dust concentration, with similar values (Fig. 5). In particular, at 2.7 kyr, about 50% of the sulphate particles (top) and chloride particles (bottom) adhere to dust, but at 27.1 kyr, the percentage rises to about 80%. The linear relationship may be useful for estimating how many insoluble dust particles potentially act as cloud condensation nuclei.

The averaged number fraction (i.e. percentage of particles) of sulphate and chloride compounds for each stage is shown in Fig. 6. Of the soluble sulphate and chloride salts, NaCl and Na_2SO_4 are the main salts, with NaCl contributing about 30% to the total chloride compounds and Na_2SO_4 contributing a similar amount to the total sulphate. This suggests that sodium compounds contribute about 60% to the total sulphate and chloride compounds. These numbers suggest that the main soluble aerosols of NaCl and Na_2SO_4 may be due to the nearby sources of sea salt and sulphuric acid. The salt content in the TD core differs from that in DF, particularly for the Holocene. For the Holocene (2.7 and 8.2 kyr), the TD ice has many NaCl particles, whereas DF has few (Iizuka et al., 2012a, 2012b).

3.3. Amount of sea-salt sulphatisation at low dust concentration during the Holocene

The main characteristic of soluble aerosols in TD ice is the high contribution of sea salt (NaCl), even during the Holocene. Here, we quantify the amount of sea salt unaffected by sulphuric acid.

To examine the amount of NaCl unaffected by H_2SO_4, we compare the molar concentrations M_{NaCl} and $M_{Na_2SO_4}$. The top of Fig. 7 shows the molar ratio of M_{NaCl} to $M_{Na_2SO_4}$. Although the dependence on dust concentration shows no significant trend, the molar ratio of most samples

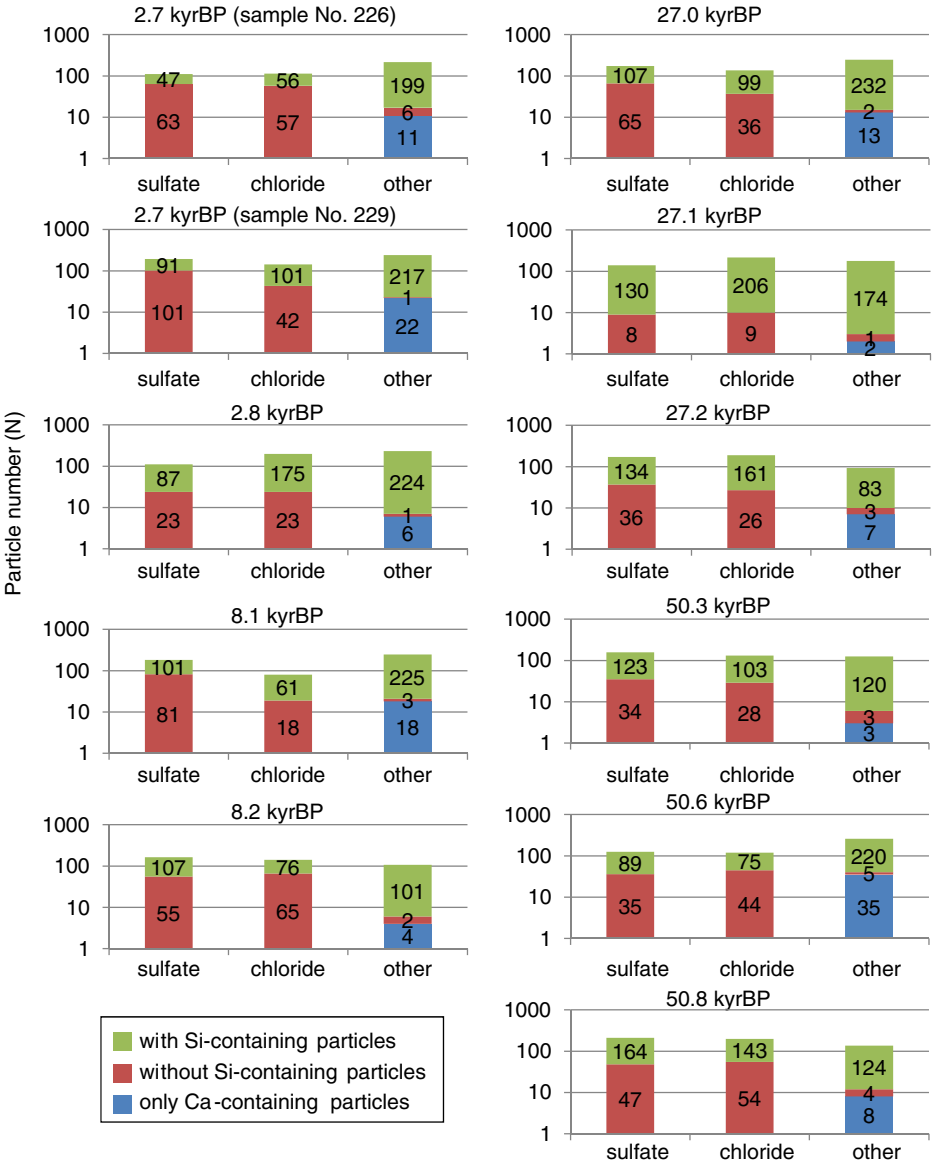

Fig. 3. Frequencies of the elemental compositions in non-volatile (post-sublimation) particles from the TD core. 'sulphate' and 'chloride' bars mean S- and Cl-containing particles. 'Other' means without sulphate and chloride particles. The green section indicates particles with Si, whereas red indicates without Si. The blue section, a special case of the red section, indicates Ca (or Ca and O) detected particles without Si, Al, S, Cl, Na and Mg. Numbers on the bars are the number of particles for the corresponding colour. The logarithmic scale is used to distinguish between blue and red sections.

exceed one, suggesting $M_{NaCl} > M_{Na_2SO_4}$. On average, this ratio at 2.7 kyr with 7.0 ppb of the lowest dust concentration is 1.53 (from 0.34 to 2.17 in each sample).

Using the ratio of 1.53 (0.34–2.17), together with the scheme described in Iizuka et al. (2012b), we calculate how much of the sodium chloride was sulphatised. In the scheme, we also use the molar ratios of NaCl to Na_2SO_4 in open seawater (14.7) and in sea ice (39.8). The molar ratios tend to decrease due to sea-salt sulphatisation during transportation from the Southern Ocean to Antarctica. The scheme can be adapted if Na^+ and Cl^- originate only from sea salt (Iizuka et al., 2012b). However, ice from the cold stage has a high dust concentration, and thus contains a certain amount of non-sea-salt soluble sodium (Bigler et al., 2006). As only the 2.7 kyr samples have a low dust concentration, we applied the scheme to only the 2.7 kyr samples.

If the salt originated in sea ice, the molar ratio would have had to decrease from 39.8 to 1.53. If we denote $[Na_2SO_4]$ (mol) at the source as k, then [NaCl] at the source

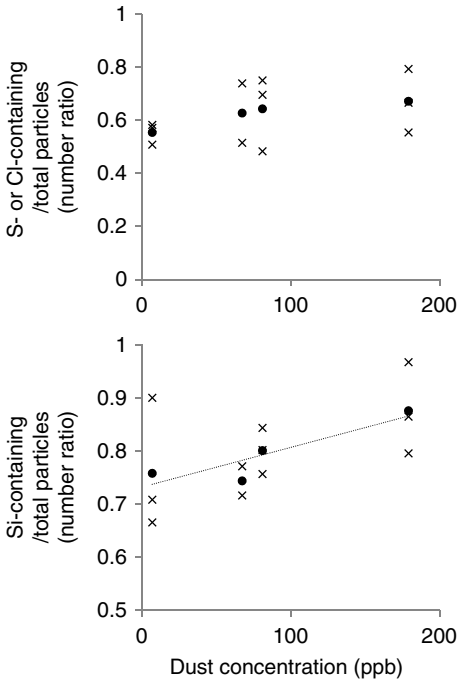

Fig. 4. Number ratios of particles with S or Cl and particles with Si for a range of dust concentrations. (top) Ratio of particles with S or Cl to total particles. (bottom) Ratio of particles with Si to total particles. Crosses are data for the 11 samples, and the black circles are averaged values of every four stages. The correlation coefficient of the regression line in Fig. 4 bottom is 0.80 (no significance level given as there were only four points).

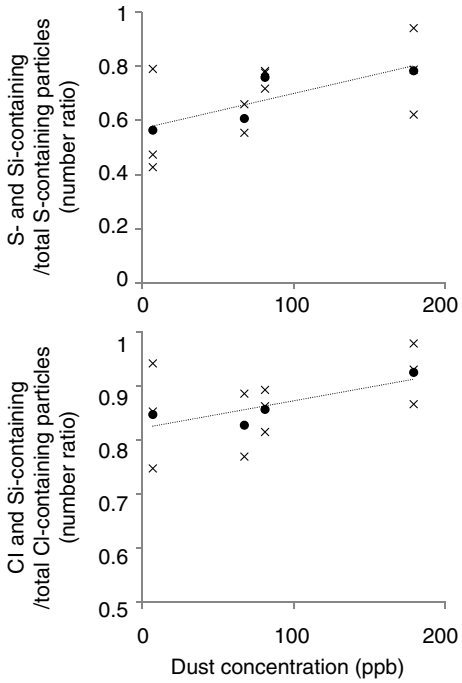

Fig. 5. Same as Fig. 4 except for particles with both S and Si and particles with both Cl and Si. (top) Ratio of particles with both S and Si to total particles. The regression-line correlation coefficient is 0.72. (bottom) Ratio of particles with both Cl and Si to total particles. The corresponding correlation coefficient is 0.73.

is $39.8k$ (mol). Similarly, if the rate of [Na_2SO_4] production is n (mol), then the amount of [NaCl] that must react is $2n$ (mol). This notation leads to the following expression:

$$\frac{[\mathrm{NaCl}]}{[\mathrm{Na_2SO_4}]} = \frac{39.8k - 2n}{k + n} = 1.53.$$

Solving this equation yields $n = 10.8k$ (mol). As a result, in the 2.7 kyrBP ice, we can express [NaCl] as $18.1k$ ($= 39.8k - 2 \times 10.8k$). As the amount of [NaCl] at the source is $39.8k$, then about 54.5% of the initial sodium chloride is removed by sulphatisation in the atmosphere and/or after precipitation. For all samples, the values varied from 45.3 to 85.9%.

If the salt instead originated from the open sea, the same analysis predicts that [NaCl] at the source should be $14.7k$ (mol). The [NaCl] values at the source and Holocene ice are $14.7k$ and $7.24k$, respectively. Thus, in this scenario, about 50.8% (range: 40.9–84.8%) of the initial sea salt is removed by sulphatisation.

In both cases of open seawater and sea ice, the average ratio shows that about half of the sea-salt particles are preserved in TD Holocene ice as marine primary aerosols. Compared to DF surface snow, which has about 90% of sea salt sulphatised (Iizuka et al., 2012b), sea salts reaching the depths of TD ice are less affected by secondary aerosol formation in the atmosphere.

A reason for the difference may be related to the higher dust contribution in TD ice than that at DF and other sites further inland (Albani et al., 2012). The argument goes as follows. The dust contribution has a fluctuation that correlates well to that of calcium-ion concentration (Wolff et al., 2006). And the calcium ion in ice promotes calcium sulphate formation (Sakurai et al., 2011), which restrains the sea-salt sulphatisation. The result would cause high NaCl and low Na_2SO_4 (Röthlisberger et al., 2003). In support, we find a positive relation between the number fraction of NaCl particles and dust concentrations (ppb) (Fig. 7). In this way, the higher dust concentration at TD may help explain the greater preservation of NaCl at TD. Although this can be adapted for 8.2 kyr (and for colder stages such as 27.1 and 50.6 kyrs) in TD ice, it does not apply to the 2.7-kyrBP ice, which has lower dust concentrations that more nearly equal those further inland.

Ion concentrations of Ca^{2+}, Na^+, Cl^- and SO_4^{2-} in pit snow in TD and DF sites are published (Severi et al., 2009, Iizuka et al., 2004). Both sites have extremely low Ca^{2+} concentration compared to the other three ions. In equivalent concentration, Cl^- and SO_4^{2-} are 1.40 and 1.05 times that of Na^+ at TD from 1979 to 2003, respectively. At the

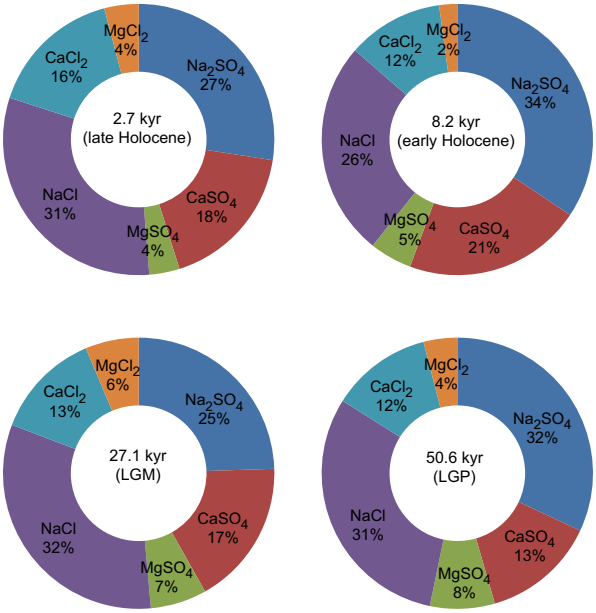

Fig. 6. Sulphate and chloride compounds at 2.7, 8.2, 27.1 and 50.6 kyrBP in TD ice samples. The early and late Holocene data are averages of two and three samples. For the two LGP stages (27 and 50 kyr BP) the averages are over three samples each.

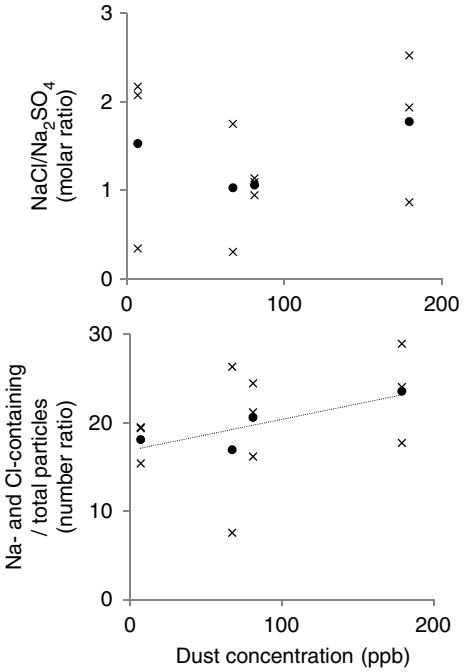

Fig. 7. Same as Fig. 4 except for the molar ratio of NaCl/Na_2SO_4 and the particles with both Na and Cl. (top) Molar ratio of NaCl/Na_2SO_4. (bottom) Ratio of particles with both Na and Cl to total particles. The correlation coefficient of the regression line is 0.72.

DF site, Cl^- and SO_4^{2-} are 1.58 and 2.11 times that of Na^+ from 1962 to 1999, respectively. Both sites have excess Cl^- and SO_4^{2-} compared with Na^+ in equivalent concentration. If the ion-deducing method of soluble-salt concentration (Iizuka et al., 2008) is applied, almost all snow at both sites contains Na_2SO_4 but not NaCl. This deduced salt concentration contrasts with the result of the molar ratios of NaCl to Na_2SO_4 (1.53 on the average) at TD 2.7 kyr, although this agrees well with the soluble-salt composition at DF. If we assume that the 2.7-kyr ice has the same ion balance among Ca^{2+}, Na^+, Cl^- and SO_4^{2-} as that in the surface snow, the above implies that the TD 2.7-kyr ice has an unstable condition for sea-salt sulphatisation. The unstable condition is probably due to a relative lack of contact between NaCl particles and H_2SO_4 acid.

Concerning the low sulphatisation in the 2.7-kyrBP TD ice, the analyses suggest that the NaCl particles had less contact with H_2SO_4 acid than particles reaching regions further inland such as DF. The simplest explanation is pre-depositional: the marine-sourced aerosol has less time to react before reaching TD. However, there are post-depositional factors to consider as well. The higher accumulation rate at TD leads to less sublimation of snow and acid at the surface snow than that at DF (Kameda et al., 2008). Less snow sublimation means that less H_2SO_4 and NaCl migrate from the inside to the surface of the snow crystals, thus providing less chance of contact between the acid and salt. On the other hand, the higher snow temperature at TD should promote the diffusion of H_2SO_4 in snowpack and increase the surface-snow sublimation rate. Which process most affects snow sublimation is presently unknown. Nevertheless, the possible mechanisms that increase the NaCl-particle survival are the shorter time to react before reaching TD and the lower sublimation of snow and acid. Both pre-depositional and post-depositional factors may play a role.

3.4. *Soluble calcium composition in TD ice core*

We now consider calcium compounds. Just 2.93% of the particles in all 11 TD samples are both categorised as 'other', meaning without S and Cl, and also do not have Si (i.e. the red and blue sections of the 'other' bar in Fig. 3). Within this category, 80.6% of the particles had Ca but did not contain Al, S, Cl, Na and Mg (blue bars in Fig. 2). Unless they contain both Al and O, these Ca particles are probably soluble solid material (Iizuka et al., 2009). Such soluble Ca-compounds are assumed to be calcium nitrate or calcium carbonate (Iizuka et al., 2008) because the EDS method poorly detects light elements such as C and N. Thus, calcium nitrate or calcium carbonate may be preserved in the TD ice sample. This result supports the finding of Sala et al. (2008) that calcium carbonates are

detected in TD ice. Due to a high calcite loss by sulphatisation during long-distance transport (Iizuka et al., 2008), local rock outcrops at high elevation in the Transantarctic Mountains (e.g. Francis and Hill, 1996) may be a potent source of calcite in TD ice.

4. Conclusion

We used the sublimation method (Iizuka et al., 2009) to examine about 5,000 particles of non-volatile aerosols in the TD ice core. The main soluble salts were NaCl and Na_2SO_4, indicating that the TD ice contains many primary aerosols consisting largely of sea salts. According to the evaluation of molar ratio of NaCl to Na_2SO_4, about half of the Holocene sea-salt did not undergo sulphatisation at 2.7 kyrBP. One possible reason is that the marine-sourced aerosol has less time to react before reaching TD compared to inland Antarctica. Another possible reason is that higher accumulation rates at TD reduces the snow sublimation rate, leading to less exposure of non-volatile materials (acid and salt) at the surface snow. Colder stages of 8.2, 27.1 and 50.6 kyrs in TD ice have higher dust contributions in TD ice. The dust (calcium ion) in ice restrains the sea-salt sulphatisation. Thus, colder stages have an additional mechanism for producing relatively high NaCl and low Na_2SO_4 levels.

Dust concentration shows a positive correlation with a number of variables we have derived from our measurements: the ratios of (1) Si-containing to total particles; (2) S- and Si- containing to S-containing particles; (3) Cl- and Si-containing to Cl-containing particles; and (4) NaCl to total particles. Because of relations (2) and (3), one may use the dust concentration to estimate how many insoluble dust particles have the potential of acting as cloud condensation nuclei. Because of relation (4), the dust concentration may be useful for estimating the sea-salt contribution to the total soluble and insoluble aerosols. Also, in particles without Si, S and Cl, most had detectable levels of only Ca (or only Ca and O), implying that the TD ice contains soluble Ca-materials such as calcium nitrate and calcium carbonate.

5. Acknowledgment

We thank the logistic and drilling TALDICE team. TALDICE, a joint European programme led by Italy, is funded by national contributions from Italy, France, Germany, Switzerland and the United Kingdom. The main logistical support was provided by Programma Nazionale di Ricerche in Antartide (PNRA) at Talos Dome. This is TALDICE publication no. 31.

This study was also supported by Scientific Research (A) grant number 23680001 provided by the Ministry of Education, Culture, Sports, Science and Technology (MEXT) and Japan's Society for the Promotion of Science (JSPS), and also by a Grant for Joint Research Program of the Institute of Low Temperature Science, Hokkaido University. This work was also supported by the JSPS Institutional Program for Young Researcher Overseas Visits. This work is a contribution of HOLOCLIP, a joint research project of ESF PolarCLIMATE programme, funded by national contributions from Italy, France, Germany, Spain, Netherlands, Belgium and the United Kingdom. In Italy HOLOCLIP is funded by PNRA. This is HOLOCLIP publication no. 17.

References

Albani, S., Delmonte, B., Maggi, V., Baroni, C., Petit, J.-R. and co-authors. 2012. Interpreting last glacial to Holocene dust changes at Talos Dome (East Antarctica): implications for atmospheric variations from regional to hemispheric scales. *Clim. Past*. **8**, 741–750. DOI: 10.5194/cp-8-741-2012.

Andreae, M. O. 1995. Climatic effects of changing atmospheric aerosol levels. In: *Future Climates of the World: A Modeling Perspective World Survey of Climatology, Volume 16* (ed. A. Henderson-Sellers). Elsevier, Amsterdam, pp. 347–398.

Bigler, M., Röthlisberger, R., Lambert, F., Stocker, T. F. and Wagenbach, D. 2006. Aerosol deposited in East Antarctica over the last glacial cycle: detailed apportionment of continental and sea-salt contributions. *J. Geophys. Res.* **111**(D08205), 1–14.

Buiron, D., Chappellaz, J., Stenni, B., Frezzotti, M., Baumgartner, M. and co-authors. 2011. TALDICE-1 age scale of the Talos Dome deep ice core, East Antarctica. *Clim. Past*. **7**, 1–16. DOI: 10.5194/cp-7-1-2011.

Delmonte, B., Andersson, P. S., Hansson, M., Schöberg, H., Petit, J. R. and co-authors. 2008. Aeolian dust in East Antarctica (EPICA-Dome C and Vostok): provenance during glacial ages over the last 800 kyr. *Geophys. Res. Lett*. **35**(L07703), 1–6. DOI: 10.1029/2008GL033382.

Delmonte, B., Andersson, P. S., Schoberg, H., Hansson, M., Petit, J. R. and co-authors. 2010a. Geographic provenance of aeolian dust in East Antarctica during Pleistocene glaciations: preliminary results from Talos Dome and comparison with East Antarctic and new Andean ice core data. *Quat. Sci. Rev*. **29**, 256–264. DOI: 10.1016/j.quascirev.2009.05.010.

Delmonte, B., Baroni, C., Andersson, P. S., Narcisi, B., Salvatore, M. C. and co-authors. 2013. Modern and Holocene aeolian dust variability from Talos Dome (Northern Victoria Land) to the interior of the Antarctic ice sheet. *Quat. Sci. Rev*. **64**, 76–89.

Delmonte, B., Baroni, C., Andersson, P. S., Schoberg, H., Hansson, M. and co-authors. 2010b. Aeolian dust in the Talos Dome ice core (East Antarctica, Pacific/Ross Sea sector): Victoria Land versus remote sources over the last two climate cycles. *J. Quat. Sci*. **25,** 1327–1337. DOI: 10.1002/jqs.1418.

Delmonte, B., Basile-Doelsch, I., Petit, J.-R., Maggi, V., Revel-Rolland, M. and co-authors. 2004a. Comparing the Epica and Vostok dust records during the last 220,000 years: stratigraphical correlation and provenance in glacials periods. *Earth. Sci. Rev*. **66**, 63–87.

Delmonte, B., Petit, J. R., Andersen, K. K., Basile-Doelsch, I., Maggi, V. and co-authors. 2004b. Dust size evidence for opposite regional atmospheric circulation changes over East Antarctica during the last climatic transition. *Clim. Dyn.* **23**, 427–438. DOI: 10.1007/s00382-004-0450-9.

Francis, J. E. and Hill, R. S. 1996. Fossil plants from the pliocene sirius group, transantarctic mountains: evidence for climate from growth rings and fossil leaves. *PALAIOS*. **11**(4), 389–396.

Fujii, Y., Kohno, M., Matoba, S., Motoyama, H. and Watanabe, O. 2003. A 320 k-year record of microparticles in the Dome Fuji, Antarctica ice core measured by laser-light scattering. *Mem. Natl. Inst. Polar Res., Spec. Issue*. **57**, 46–62.

Iizuka, Y., Fujii, Y., Hirasawa, N., Suzuki, T., Motoyama, H. and co-authors. 2004. SO42- minimum in summer snow layer at Dome Fuji, Antarctica and the probable mechanism. *J. Geophys. Res.* **109**(D04307). DOI: 10.1029/2003JD004138.

Iizuka, Y., Horikawa, S., Sakurai, T., Johnson, S., Dahl-Jensen, D. and co-authors. 2008. A relationship between ion balance and the chemical compounds of salt inclusions found in the GRIP and Dome Fuji ice cores. *J. Geophys. Res.* **113**(D07303). DOI: 10.1029/2007JD009018.

Iizuka, Y., Miyake, T., Hirabayashi, M., Suzuki, T., Matoba, S. and co-authors. 2009. Constituent elements of insoluble and nonvolatile particles during the last glacial maximum of the Dome Fuji ice core. *J. Glaciol.* **55**(191), 552–562.

Iizuka, Y., Tsuchimoto, A., Hoshina, Y., Sakurai, T., Hansson, M. and co-authors. 2012b. The rates of sea salt sulfatization in the atmosphere and surface snow of inland Antarctica. *J. Geophys. Res.* **117**(D04308). DOI: 10.1029/2011JD01637.

Iizuka, Y., Uemura, R., Motoyama, H., Suzuki, T., Miyake, T. and co-authors. 2012a. Sulphate-climate coupling over the past 300,000 years in inland Antarctica. *Nature*. **490**, 81–84. DOI: 10.1038/nature11359.

Kameda, T., Motoyama, H., Fujita, S. and Takahashi, S. 2008. Temporal and spatial variability of surface mass balance at Dome Fuji, East Antarctica, by the stake method from 1995 to 2006. *J. Glaciol.* **54**(184), 107–116 (06J108).

Kawamura, K., Nakazawa, T., Aoki, S., Sugawara, S., Fujii, Y. and co-authors. 2003. Atmospheric CO2 variations over the last three glacial–interglacial climatic cycles deduced from the Dome Fuji deep ice core, Antarctica using a wet extraction technique. *Tellus*. **55B**, 126–137.

Lambert, F., Delmonte, B., Petit, J. R., Bigler, M., Kaufmann, P. R. and co-authors. 2008. Dust climate couplings over the past 800,000 years from the EPICA Dome C ice core. *Nature*. **452**, 616–619. DOI: 10.1038/nature06763.

Legrand, M. R. and Delmas, R. J. 1988. Formation of HCl in the Antarctic atmosphere. *J. Geophys. Res.* **93**(D6), 7153–7168.

Legrand, M. R., Lorius, C., Barkov, N. I. and Petrov, V. N. 1988. Vostok (Antarctica) ice core: atmospheric chemistry changes over the last climatic cycle (160,000 years). *Atmos. Environ.* **22**(2), 317–331.

Petit, J. R., Jouzel, J., Raynaud, D., Barkov, N. I., Barnola, J.-M. and co-authors. 1999. Climate and atmospheric history of the past 420,000 years from the Vostok ice core, Antarctica. *Nature*. **399**, 429–436.

Pöschl, U. 2005. Atmospheric aerosols: composition, transformation, climate and health effects. *Angew. Chem. Int. Ed.* **44**, 7520–7540. DOI: 10.1002/anie.200501122.

Röthlisberger, R., Crosta, X., Abram, N. J., Armand, L. and Wolff, E. W. 2010. Potential and limitations of marine and ice core sea ice proxies: an example from the Indian Ocean sector. *Quat. Sci. Rev.* **29**, 303–312.

Röthlisberger, R., Mulvaney, R., Wolff, E. W., Hutterli, M. A., Bigler, M. and co-authors. 2003. Limited dechlorination of sea-salt aerosols during the last glacial period: evidence from the European Project for Ice Coring in Antarctica (EPICA) Dome C ice core. *J. Geophys. Res.* **108**(D16), 4526.

Sakurai, T., Ohno, H., Horikawa, S., Iizuka, Y., Uchida, T. and co-authors. 2011. The chemical forms of water-soluble microparticles preserved in the Antarctic ice sheet during Termination I. *J. Glaciol.* **57**(206), 1027–1032.

Sala, M., Delmonte, B., Frezzotti, M., Proposito, M., Scarchilli, C. and co-authors. 2008. Evidence of calcium carbonates in coastal (Talos Dome and Ross Sea area) East Antarctica snow and firn: environmental and climatic implications. *Earth. Planet. Sci. Lett.* **271**(1–4), 43–52. DOI: 10.1016/j.epsl.2008.03.045.

Schüpbach, S., Federer, U., Bigler, M., Fischer, H. and Stocker, T. F. 2011. A refined TALDICE-1a age scale from 55 to 112 ka before present for the Talos Dome ice core based on high-resolution methane measurements. *Clim. Past*. **7**, 1001–1009. DOI: 10.5194/cp-7-1001-2011.

Severi, M., Becagli, S., Castellano, E., Morganti, A., Traversi, R. and co-authors. 2009. Thirty years of snow deposition at Talos Dome (Northern Victoria Land, East Antarctica): chemical profiles and climatic implications. *Microchem. J.* **92**, 15–20.

Stenni, B., Buiron, D., Frezzotti, M., Albani, S., Barbante, C. and co-authors. 2011. Expression of the bipolar seesaw in Antarctic climate records during the last deglaciation. *Nature. Geosci.* **4**, 46–49. DOI: 10.1038/NGEO1026.

Watanabe, O., Kamiyama, K., Motoyama, H., Fujii, Y., Igarashi, M. and co-authors. 2003. General tendencies of stable isotopes and major chemical constituents of the Dome Fuji deep ice core. *Mem. Natl. Inst. Polar Res., Spec. Issue,* **57**, 1–24.

Wolff, E. W., Fischer, H., Fundel, F., Ruth, U., Twarloh, B. and co-authors. 2006. Southern Ocean sea-ice extent, productivity and iron flux over the past eight glacial cycles. *Nature*. **440**, 491–496. DOI: 10.1038/nature04614.